



Tornado damage analysis of a forest area using site survey observations, radar data and a simple analytical vortex model

Joan Bech ^{a,*}, Miquel Gayà ^b, Montserrat Aran ^a, Francesc Figuerola ^a, Jéssica Amaro ^a, Joan Arús ^c

^a Meteorological Service of Catalonia, Berlín 38, Barcelona E- 08029, Spain

^b Instituto Nacional de Meteorología, CMT Illes Balears, Palma de Mallorca, Spain

^c Instituto Nacional de Meteorología, CMT Catalunya, Barcelona, Spain

ARTICLE INFO

Article history:

Received 3 December 2007

Revised 12 October 2008

Accepted 14 October 2008

Keywords:

Wind damage

Weather radar

Vortex model

Tornado life cycle

ABSTRACT

This paper deals with the application of a methodology to characterize tornado damage in forests based on a simple two dimensional stationary tornado vortex to describe the surface wind field. The basic vortex model is built over the traditional approach of a combined Rankine velocity profile with radial and azimuthal components plus a constant translational field. Several additions are considered such as producing theoretical swath patterns including absolute velocity values (to compare more easily with Fujita damage rating) or using radar data to estimate the translational speed of the vortex. The methodology is demonstrated with the Castellcir tornado that took place in Catalonia (NE Spain) on the 18th October 2006. The site survey indicated a 4 km path and 260 m maximum width as well as F2 damage. Further analysis suggests the existence of three stages in the tornado life cycle: 1) an organising stage with predominantly inflow pattern; 2) a mature stage with predominant tangential circulation of the vortex and maximum damage and width path –possibly influenced by the complex topography of the terrain–, and 3) a dissipating stage showing weakening and narrowing of the damage path but no outflow patterns. The methodology also helped to confirm the tornadic character of the damage discarding possible microbursts in some parts of the area surveyed.

© 2008 Elsevier B.V. All rights reserved.

1. Introduction

Site surveys of strong convective-wind events affecting densely populated urban or periurban locations normally differ substantially from those in rural or forest areas scarcely populated. Even for short-lived and weak tornadoes or downbursts –i.e. with associated damage weaker than F2 in the Fujita scale (Fujita, 1981)– the effects in man-made structures found in post-event surveys usually provide valuable information to determine the extent, intensity and causing mechanism of the damage observed. This information can seldom be obtained by standard operational observing systems (conventional surface observations, satellite, radar, etc.) because of the relatively small temporal and spatial scales

involved as discussed by Fujita (1981) or in a recent review by Bluestein (2007). Moreover, the increasing availability of digitally recorded observations (pictures or videos) by spotter or casual witnesses in populated areas may supply a huge amount of additional information which, among other things, can help to discriminate if a particular event was tornadic or not.

The situation in scarcely populated forest areas is completely different: generally the evidence of damage is restricted to the effects on vegetation and the ground. This limits substantially the assessment of the damage with the Fujita scale which was developed originally to be applied to man-made structures. The new updated version, the Enhanced Fujita scale (EF scale) recently adopted in the US (Doswell et al., 2007), tries to overcome this limitation by describing in more detail the effects on vegetation, though still much less precisely than to artificial structures: 2 of the newly introduced 28 damage indicators are devoted to trees;

* Corresponding author. Tel.: +34 93 567 60 90; fax: +34 93 567 61 02.
E-mail address: jbech@meteo.cat (J. Bech).

the rest to man-made structures (see [TTU, 2006](#) for more details). However the effects of tornadoes over forest areas have been studied since a long time ago, as demonstrated by the pioneering studies in Europe by Alfred [Wegener \(1917\)](#) or, somewhat later, by Johannes Letzmann, as reported in detail by [Peterson \(1992a,b\)](#). Other examples of studies examining the effects of tornadoes in trees are the post-event analysis of [Hall and Brewer \(1959\)](#) and [Fujita \(1989\)](#) or others from the point of view of the forest industry such as [Peterson and Pickett \(1991\)](#) or [Peterson \(2000\)](#). Recently [Holland et al. \(2006\)](#) suggested to include a physical model of the behaviour of trees to describe more realistically their response to strong winds. The model requires information about tree height and age and allows simulating the proportion of area affected in a forest assuming certain tornado characteristics.

The purpose of this paper is to apply and discuss a methodology to characterize damage wind patterns in forest areas, based on a classical tornado vortex model for surface winds. This approach may help in post-event analysis of convective-driven windstorms, particularly those affecting low density populated areas with little or no effects on man-made structures. Under those circumstances there is usually very limited, if any, conventional observational data, including eye witnesses, and tree damage patterns can be used as proxy data to complement site survey analysis. The methodology is illustrated examining a case study, the recent Castellcir tornado that affected the northeast of Spain, on the 18th October 2006. Inclusion of a physical tree model is discarded in this case, given the lack of additional information about trees required for such model.

The organization of the rest of the paper is as follows. [Section 2](#) describes the surface wind model considered, including a simple tornado vortex, the associated damage path swaths and the details of the implementation. [Section 3](#) deals with the case study, explaining the site survey data collection and analysis and the complementary information obtained from the methodology suggested. Finally the paper is completed with a summary and conclusions of the study presented.

2. A simple tornado model and associated damage in forests

The complexity of tornado vortices has been studied in the past with laboratory experiments ([Dessens, 1972](#); [Church et al., 1979](#)), numerical simulations focusing in dynamical aspects ([Lewellen, 1993](#); [Grasso and Cotton, 1995](#)), and, more recently, observational studies mainly based in high-resolution Doppler weather radar (see for example [Burgess et al., 2002](#); [Wurman, 2002](#); [Wakimoto et al., 2003](#); [Lee and Wurman, 2005](#); [Bluestein et al., 2003, 2004, 2007](#)).

In the following subsections a vortex model to describe the tornado wind field near the ground and the associated swath damage are introduced.

2.1. Surface vortex model

Despite the complexity of the wind field associated with tornado vortices they have been traditionally approximated with relatively simple models. The classical simplest approach to describe a stationary two-dimensional tornado vortex near the ground is the combined Rankine vortex ([Fig. 1](#)). In this

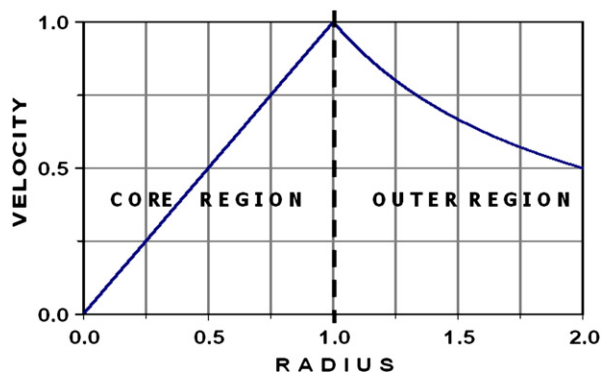


Fig. 1. Combined Rankine vortex non-dimensional velocity profile. In the core region the speed increases linearly with the radius (solid body rotation). After the radius of maximum speed ($R = 1.0$), in the outer region the speed decreases hyperbolically.

model two regions in the wind field can be distinguished: a core region and an outer region. In the core region the profile of the tangential velocity increases linearly from the centre of the vortex, with null velocity, to a maximum value in radius R , the so-called radius of maximum wind speed (MWS). Note that the linear increase is equivalent to a solid-body rotation regime were the angular velocity is constant. In the outer region the speed decreases hyperbolically due to friction with the environment surrounding the vortex of the core region. This simple model has the advantage of providing an analytical description of the wind field in terms of only two parameters, MWS and R . However it should be used with caution as it is clear that it is an approximation; i.e. tornado vortices present more complex circulations (three-dimensional, etc.) and are not stationary.

An additional sophistication consists in considering a similar velocity profile for the radial component of the wind velocity vector. This allows introducing non-azimuthal components which can describe in simple terms inflow or outflow from the vortex centre. Moreover, assuming that the tornado vortex is moving horizontally to a given direction and speed, a constant field may be added to the radial and tangential components. As discussed later, this was already considered in the studies by Letzmann ([Peterson, 1992a](#)).

The velocity profile described above can be seen as a particular case of a more general velocity profile where the speed $V(r)$, written as a function of distance to the vortex centre r , varies according to:

$$V(r) = MWS(r/R)^\gamma \quad \text{when } r \leq R,$$

$$V(r) = MWS(r/R)^\beta \quad \text{when } r > R,$$

so the combined Rankine model described earlier would be a particular case where β is equal to -1 and γ is equal to 1 . For example [Wurman et al. \(2007\)](#) report tornados exhibiting values of β equal to -0.6 according to high resolution Doppler radar measurements. A more complex yet realistic model of the profile is given by the Burgers-Rott vortex which is an exact solution of the Navier Stokes equation and presents a smooth transition between the core and the outer zone. [Tanamachi et al. \(2007\)](#) found good agreement between high resolution Doppler radar measurements and this model.

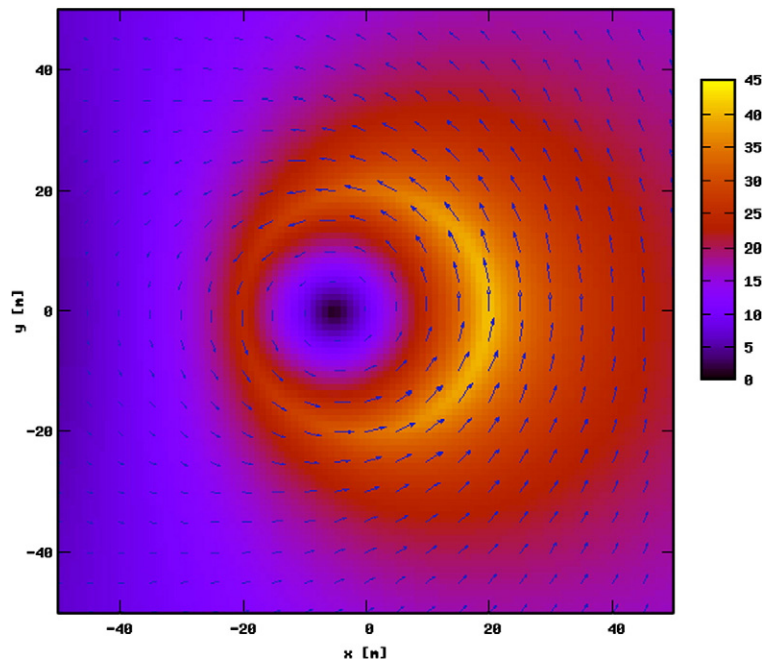


Fig. 2. Modelled surface wind field obtained with a Rankine vortex model approach with purely tangential flow and also a northern uniform component. The radius of maximum wind speed is 20 m and the speed is represented in m/s.

In this study the simple approach given by the combined Rankine vortex model is adopted considering both tangential and radial components with the same radius of maximum speed and an additional constant wind field to describe the translation of the tornado vortex. The limitations of this approximation are balanced by its simplicity as has been recognized by other authors simulating tornado vortices (see for example Holland et al., 2006; Wurman et al., 2007).

Fig. 2 shows an example of wind field obtained by combining a tangential wind component given by a combined Rankine vortex model and constant northward flow. As a starting point the radial component is omitted in this example. Note the calm area to the left of the vortex centre and the crescent pattern in the right part, where the tangential flow is added to the northern translational component.

As studied in detail by Letzmann (Peterson, 1992a; Dotzek et al., 2008), two dimensionless quantities can be used to fully characterize wind patterns of this approach: the ratio G between the rotational and translational components of the wind vector, and the angle α between radial and tangential components of the vortex field, sometimes called deflection angle. The angle α is taken from a radial initially pointing to the centre of the vortex (0°) and increasing in clockwise direction: 0° (pure radial inflow), -90° (anticlockwise pure tangential flow, i.e. cyclonic in the northern hemisphere), -180° (pure radial outflow), etc.

As recognized by Letzmann (Peterson, 1992a) the advantage of using these parameters is that the wind patterns of the isotach field are independent of the absolute velocities of rotation and translation, but it depends only of their ratio G and the angle α between the radial and tangential components. To take into account also the absolute values of the

wind speed an additional quantity must be included. To facilitate the comparison of simulated patterns and observed damage one can use the absolute maximum wind speed at radius R (resulting from the addition of the vortex speed and the translational component), for example expressed in terms of the Fujita scale equivalent wind speed (e.g., $F_{x,y}$). For instance Fig. 1 corresponds to G equal to 4, α equal to -90° and F1.5.

2.2. Damage path swath

After presenting the main elements of the wind field of the vortex model adopted in this study, the associated damage path swath is briefly discussed here, specifically for tornadoes in forests.

Except for stationary or very slow moving tornadoes, damage patterns can not be directly compared with instantaneous modelled wind fields such as that shown in Fig. 2 (see Peterson, 1992a, Fig. 7, for an example). Instead, the observed damage path swath, for instance fallen trees, must be compared with the pattern of maximum wind vectors perpendicular to the direction of movement of the modelled vortex. This implies the assumption that fallen trees are oriented according to the instantaneous wind field. Another implicit hypothesis is that the modelled wind is necessarily a lower mark of the damage caused. However, this is a general limitation of estimating the wind speed from the damage observed.

Fig. 3 illustrates three different configurations of vortex and their associated path swaths. The three cases are modelled with G equal to 4, maximum speed equivalent to F1.5 and differ only in the deflection angle α showing the case of pure inflow, pure anticlockwise tangential flow and pure

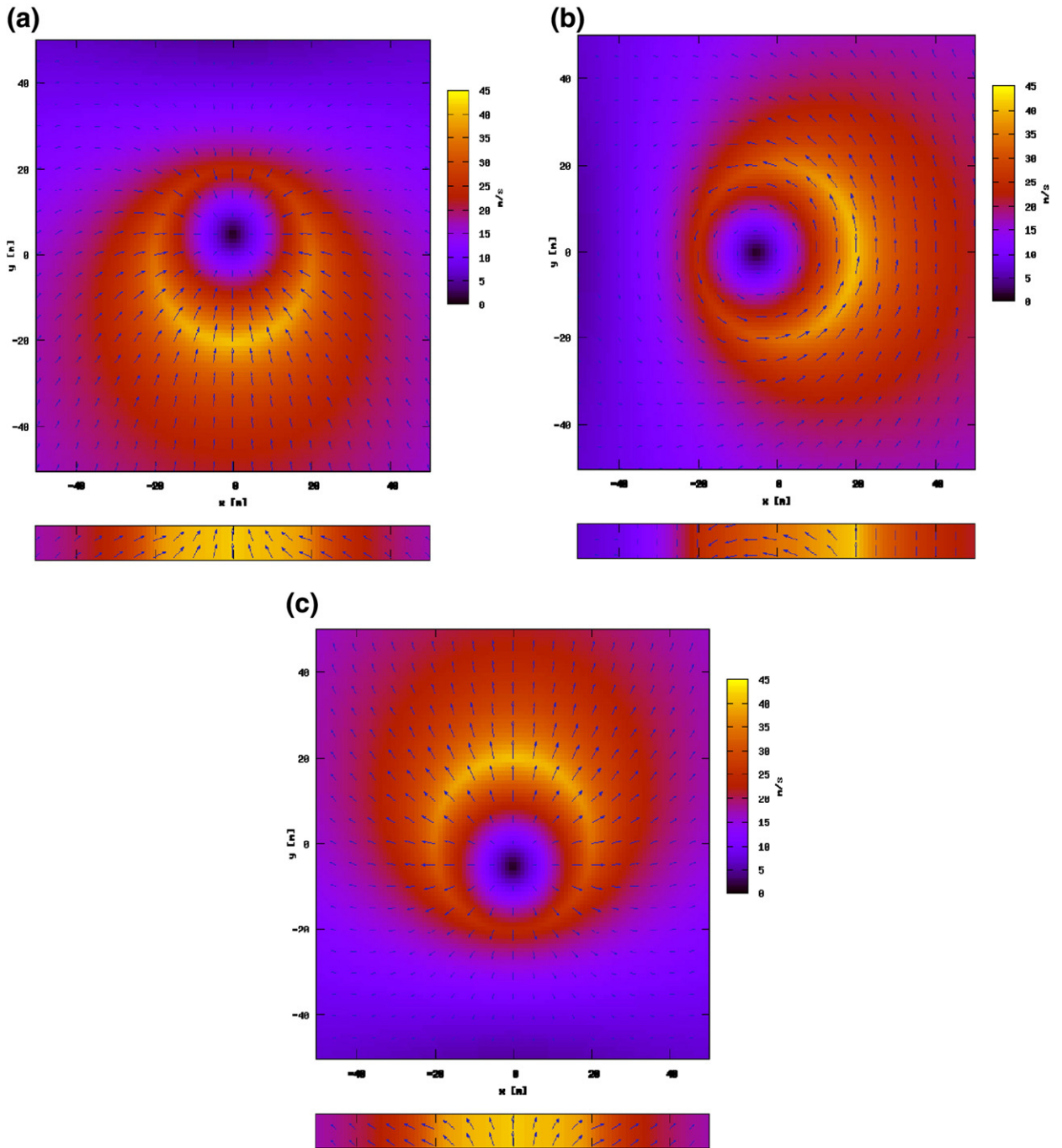


Fig. 3. Similar to Fig. 2 but here the associated swath pattern is included for each case. Note that the maximum wind speed in all three cases is $F 1.5$ and the ratio between maximum rotational and translational flow (G) is also constant and equal to 4. Each case represents different flow types of the vortex: a). pure inflow ($\alpha = 0^\circ$); a). pure tangential flow ($\alpha = -90^\circ$); a). pure outflow ($\alpha = -180^\circ$).

outflow. Note that the inflow and outflow cases exhibit a symmetric pattern of convergence and divergence, respectively. As divergent patterns can be associated with downburst effects a potential application of the comparison of observed damage with modelled patterns is helping to discriminate between tornadic and downburst cases.

The pure tangential flow shows a maximum to the right side of the path centre, a classical higher intensity damage pattern (Bunting and Smith, 1993) for cyclonic tornadoes in the northern hemisphere. In the particular case of pure tangential flow the distance of the maximum to the centre of the path indicates the radius R .

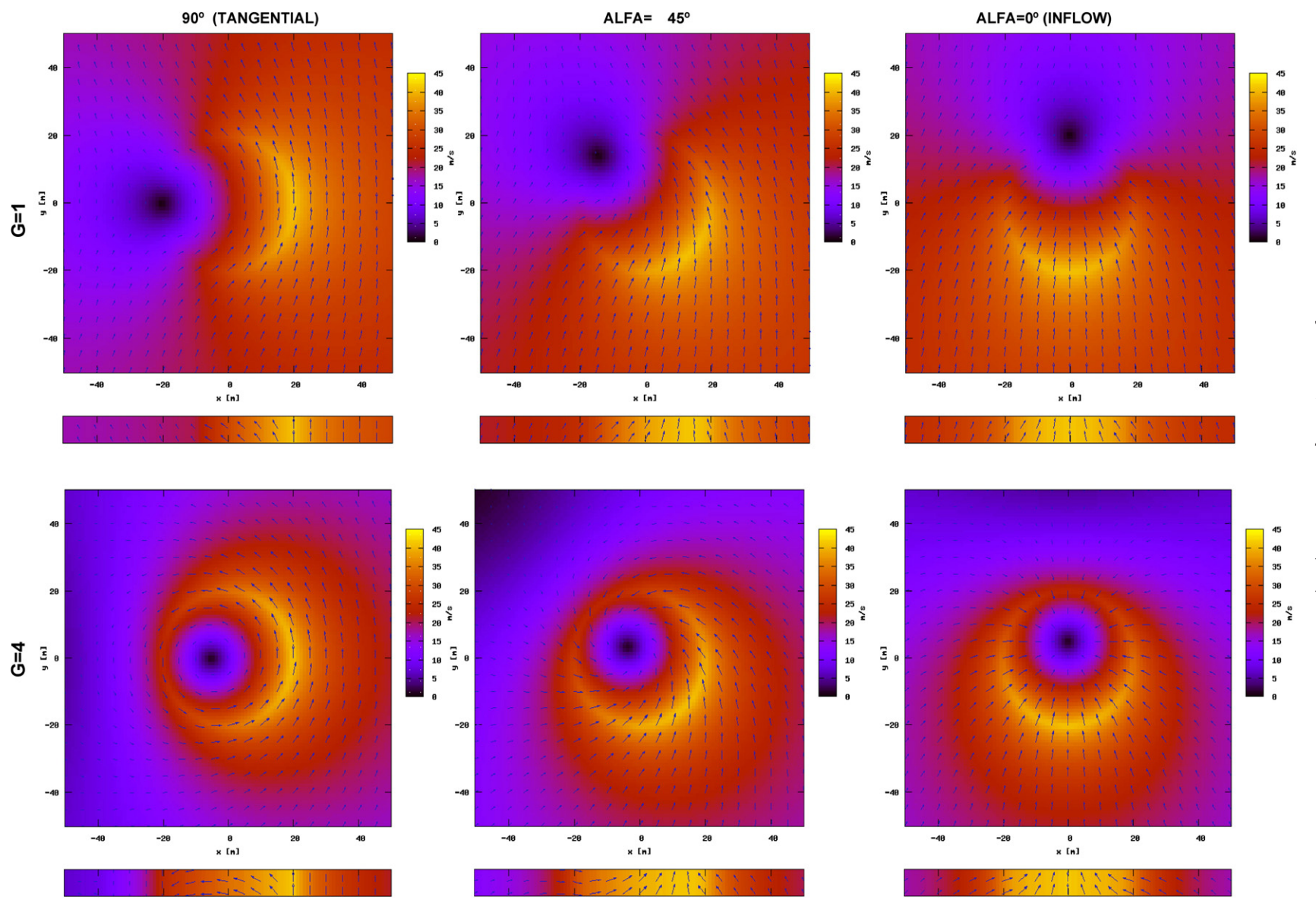


Fig. 4. Similar to Fig. 3 but here the modelled patterns are shown for G equal to 1 and 4 and for α equal to 0° , -45° and -90° .

The effect of varying the parameter G in the modelled vortex is illustrated in Fig. 4. It shows six different cases, with three possible deflection angles and two possible values for G . These modelled swath types are similar to those obtained by Letzmann (see Peterson, 1992a, Fig. 8). However here are shown with specific values of the isotach field instead of only the wind vector orientation so that it can be compared more easily with actual observed tree damage.

3. Case study: the 18th October 2006 Castellcir tornado

In this section a case of tornado damage analysis in a forest is presented. The methodology based on the vortex model described in Section 2 is demonstrated to complement the analysis. The tornado took place in Catalonia (NE Spain) the afternoon of 18th October 2006, close to the village of Castellcir. The location of Castellcir is indicated in Fig. 5. Aran et al. (2009-this issue) provides a diagnostic study of the mesoscale and synoptic conditions of the event.

Catalonia is one of the regions most prone to tornadoes in Spain according to a recent climatology by Gayà (2005) covering the period 1987 to 2005. All tornadic cases in Catalonia described in detail to date (see for example Ramis et al., 1997; Bech et al., 2007; Mateo et al., 2009) affected urban or periurban areas so this case represented a good opportunity to evaluate the methodology proposed.

Two eye-witnesses saw the Castellcir tornado at 13:30 UTC and no additional pictures or videos were taken. There were no injured people. Other evidences of strong wind effects were minor damage found in a few farms and residential houses and more widespread and intense damage in forest areas.

3.1. Radar data

Observations recorded with the Puig Bernat (PBE) C-band Doppler weather radar of the network of the Meteorological Service of Catalonia (Bech et al., 2004) indicated a SW to NE movement of the thunderstorms that afternoon. The PBE

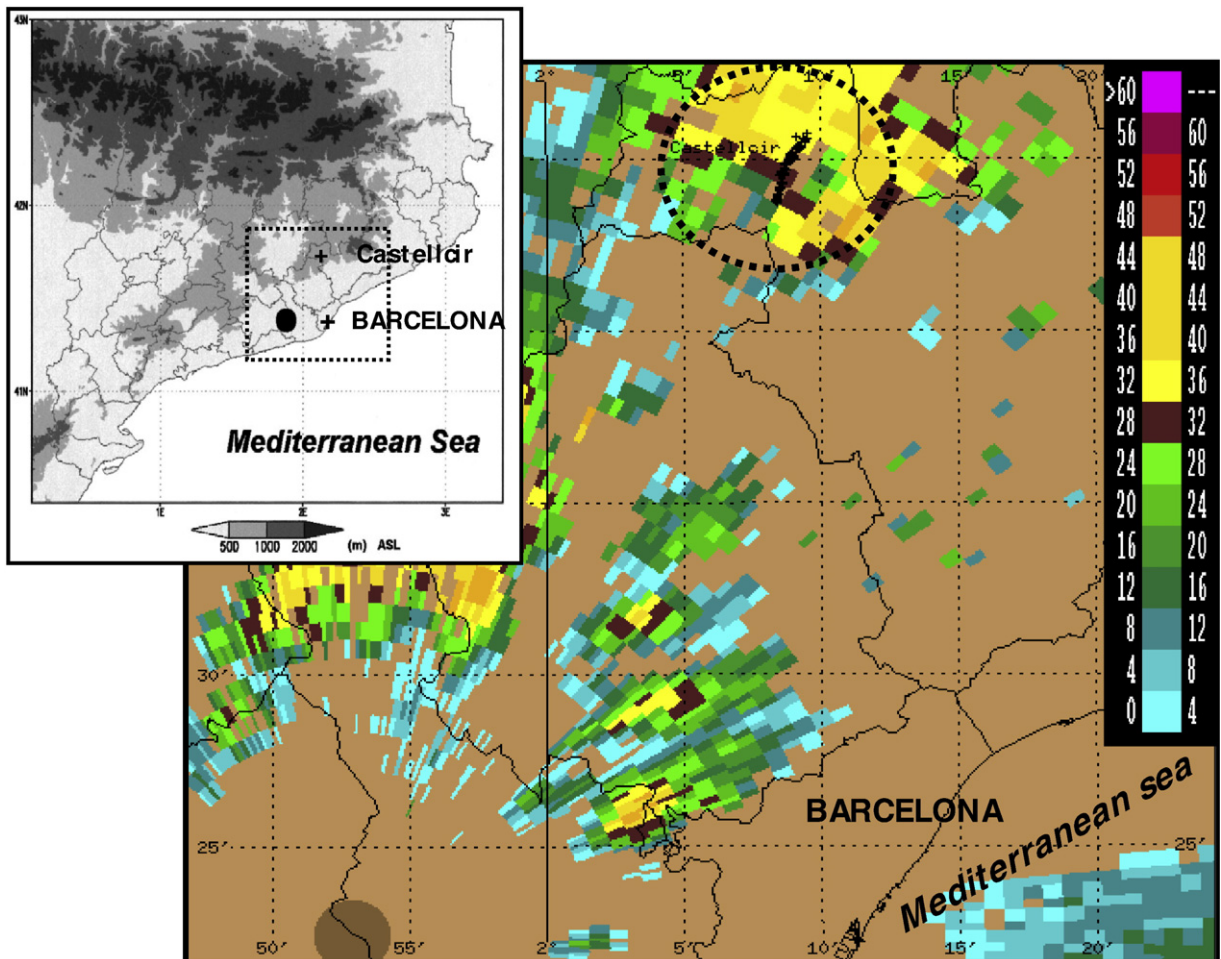


Fig. 5. Map indicating the region of the case study. The topographical map in the upper left corner shows the position of Barcelona City and Castellcir, where the tornado took place. The black dot shows the PBE radar position and the dotted square is the area of interest shown in the larger map. The larger map is a low elevation (0.7°) Plan Position Indicator image showing the radar reflectivity field at 13:32 UTC, approximately when the tornado was observed in the path marked with a dotted circle to the north. The colour scale is in dBZ. (For interpretation of the references to colour in this figure legend, the reader is referred to the web version of this article.)

radar is located about 45 km SW from Castellcir (see Fig. 5) and in this sector there is some beam blockage due to hilly terrain (Bech et al., 2003).

Base level (0.7°) Plan Position Indicator (PPI) images of the PBE radar were examined overlaid to the tornado path. A sequence of six images of radar reflectivity covering the reported time of the tornado is shown in Fig. 6. A relatively modest convective cell, in terms of extension and intensity (maximum reflectivity was 48 dBZ), crossed Castellcir in the direction of the tornado path some minutes before 13:30 UTC; a stronger and larger cell was coming behind (shown in Fig. 5, to the N of the PBE radar). The last image of the sequence of Fig. 6 (13:44 UTC) shows the second larger cell coming from the SW. As discussed in more detail in Aran et al. (2009–this issue) no clear supercell characteristics were evident in this case.

The sequence of Fig. 6 indicates that the contour line of 30 dBZ first intersected the tornado path at 13:21 UTC and left it at 13:32 UTC. This seems consistent with the time reported by the witnesses and might indicate that the tornado was at the rear part of the convective region of the cell. The estimated speed of the cell was approximately 40 km/h along the direction of the tornado path. This estimation has been used as a starting point of the translational speed of the tornado vortex model.

3.2. Site survey

A first preliminary site survey was conducted in Castellcir during the immediate days after the tornado. Information of

specific damaged forest areas was collected to prepare a more detailed survey which involved seven people and covered two complete working days plus an additional aerial survey performed with helicopter. The area covered was approximately 4×2 km² of forest and hilly terrain.

The location and orientation of representative trees was recorded using GPS and compass, complemented with pictures and local rating of damage in terms of the Fujita intensity scale (Fujita, 1981). The trees were mostly white pine (*Pinus halepensis*) and also holm oak (*Quercus ilex*) and oak (*Quercus pubescens*). Examples of different levels of damage observed are shown in Fig. 7. Special attention was devoted to determine the direction and damage of the trees, taking into account the possible effect of the terrain slope, soil type, nearby trees fallen, etc. and discarding suspect cases (for example, fallen trees in areas with very thin soil layers which may have offered little resistance, or fallen trees in very stepped slopes where the final orientation was probably not representative of the original wind direction were not considered). The final record included 144 locations of fallen trees, with 138 orientations and 130 Fujita scale ratings in 0.5 intervals.

3.3. Path details

The analysis of the data collected during the site survey indicated that the path was 4 km long, the maximum path width was 260 m and the maximum damage intensity was F2. These values seem consistent with the study of Brooks (2004) of relationships between tornado damage and length and

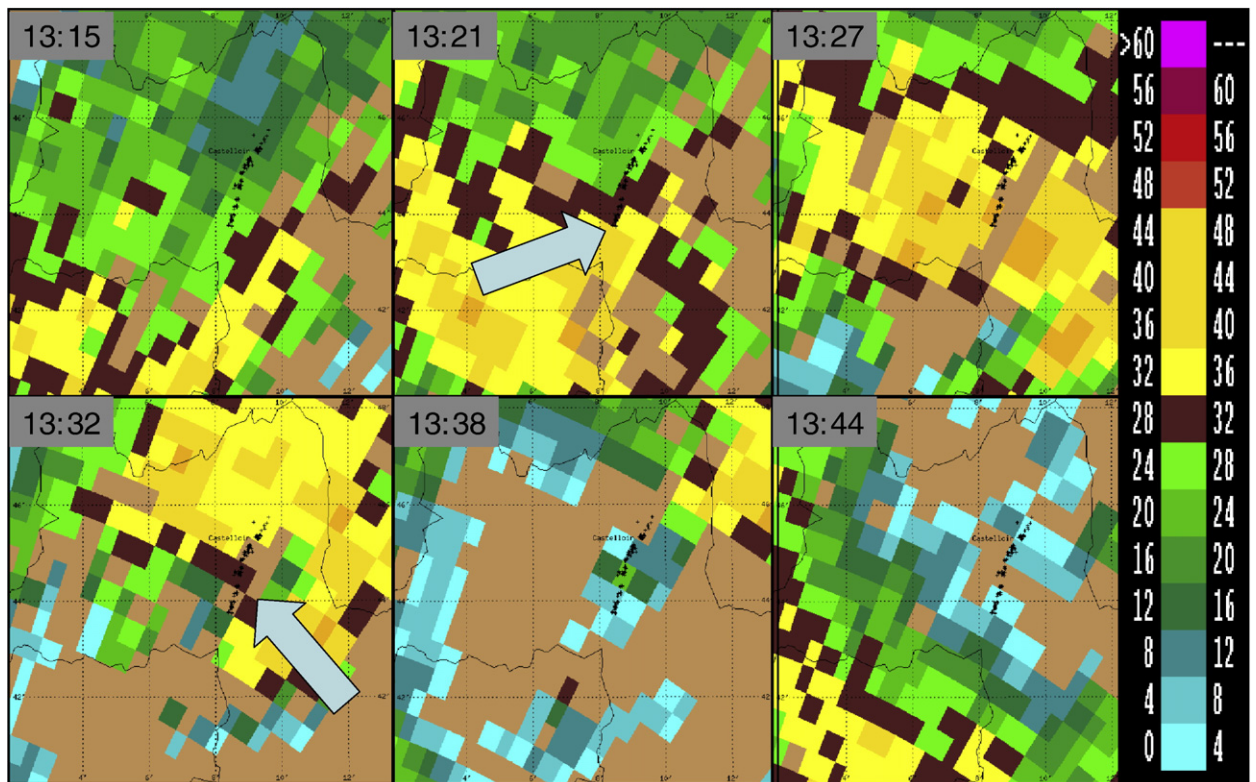


Fig. 6. Sequence of PBE low elevation (0.7°) PPI images showing the radar reflectivity field and the Castellcir tornado path. Note the intersections of the 30 dBZ contour line with the tornado path marked with arrows, indicating possible approximate times of beginning (13:21 UTC) and ending (13:32 UTC) time of the tornado. Time is indicated in UTC and the colour legend in dBZ.

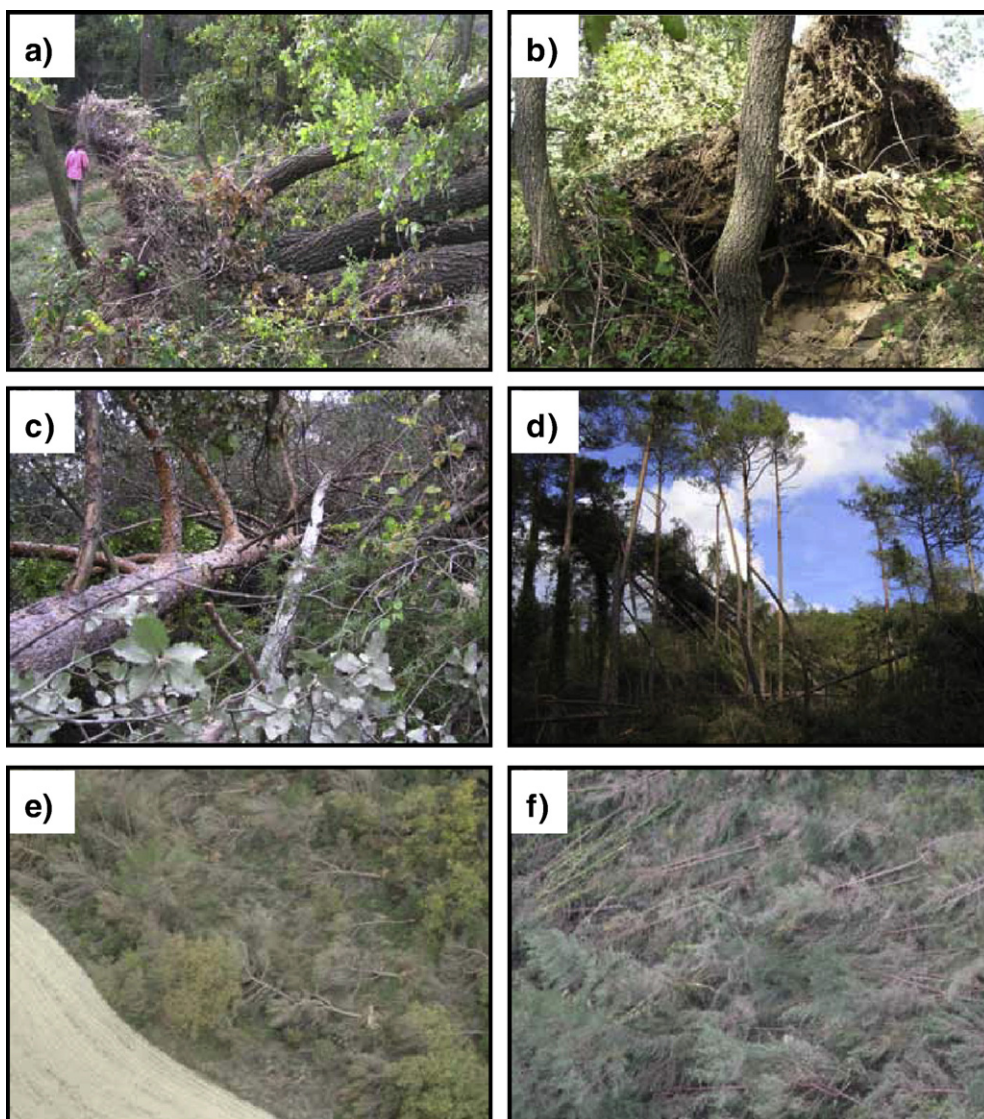


Fig. 7. Damage observed during the site survey illustrating different levels of the Fujita scale rating. a) a group of shallow-rooted fallen trees (F0), b) larger but isolated uprooted tree (F0); c) and d) larger groups of fallen or uprooted trees, indicating signs of rotation (F1); and e) and f) airborne view of two areas where all trees were fallen or uprooted (F2).

width of a database including 40,000 USA tornadoes. In particular, given a width of 260 m F2 is the most likely damage, as found in this case. The length is shorter to that expected for F2 damage but some issues have already been discussed about a possible bias to longer paths in that database (Doswell and Burgess, 1988).

Fig. 8 shows the location of the fallen trees and the estimated orientations and damage. It is also included in the estimated path centre of the tornado vortex and approximated damage contours (F0.0, F1.0 and F1.5).

The maximum damage and path width was examined in more detail dividing the area of study into 8 different square zones of $500 \times 500 \text{ m}^2$. From this analysis an estimation of the tornado life cycle was done assigning the maximum damage and width to a specific part of the tornado path, one for each

zone. Fig. 9 depicts the schematic evolution of the tornado life cycle in terms of path maximum width and damage vs path length (top panel) and the corresponding topographic profile (bottom panel).

The tornado life cycle obtained in this way, with a concurrent width and damage maximum observed at around 1.5 km from the beginning of the path, is remarkably similar to the classical tornado life cycle described by Golden and Purcell (1978) based on photogrammetric analysis of observations of the Union City tornado of 24 May 1973 which lasted about 25 min. Other studies (see for example Wakimoto and Martner, 1992; Kobayashi et al., 1996; Wakimoto et al., 2003; Bluestein et al., 2004) report similar life cycles.

The Castellcir tornado, according to the path length and the radar data, probably lasted about 5 min. During the first

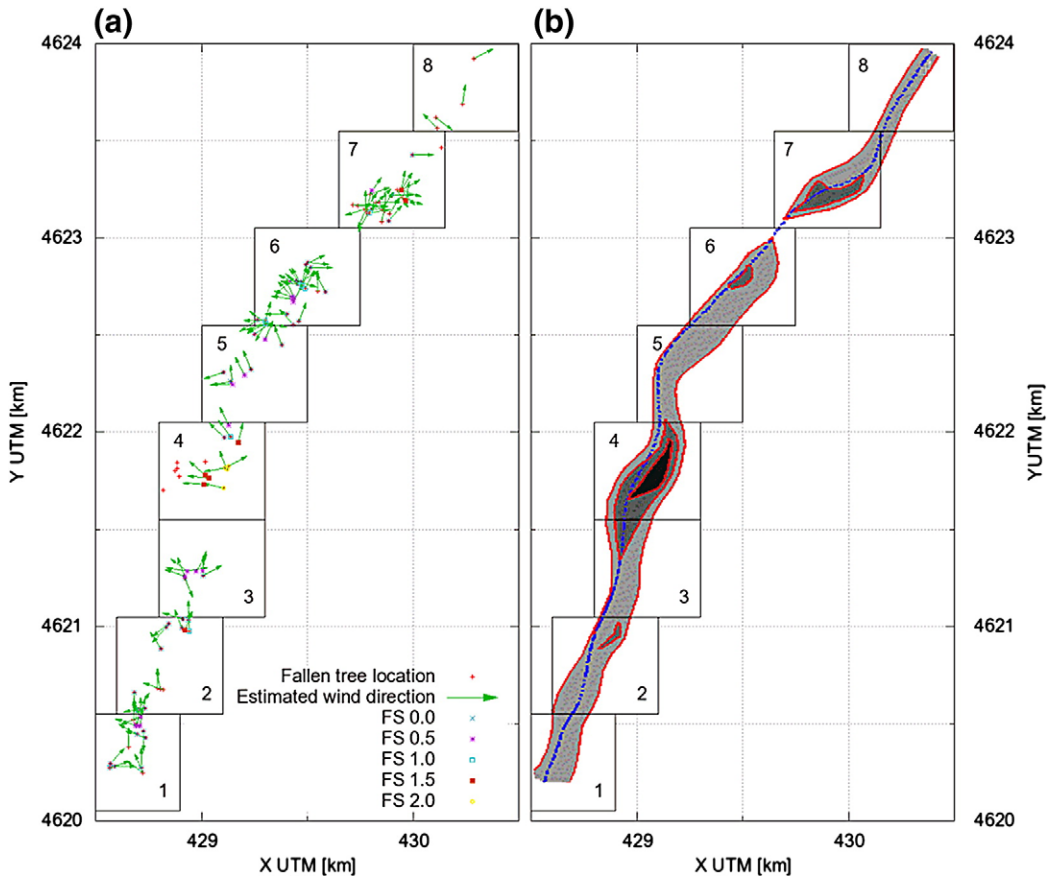


Fig. 8. a). Location of fallen trees and estimated wind direction and damage in the Fujita scale at 0.5 intervals. b). Display of the estimated path of the vortex centre and approximated damage contours (F0, F1 and F1.5). Both panels show the eight zones in which the region of study was divided.

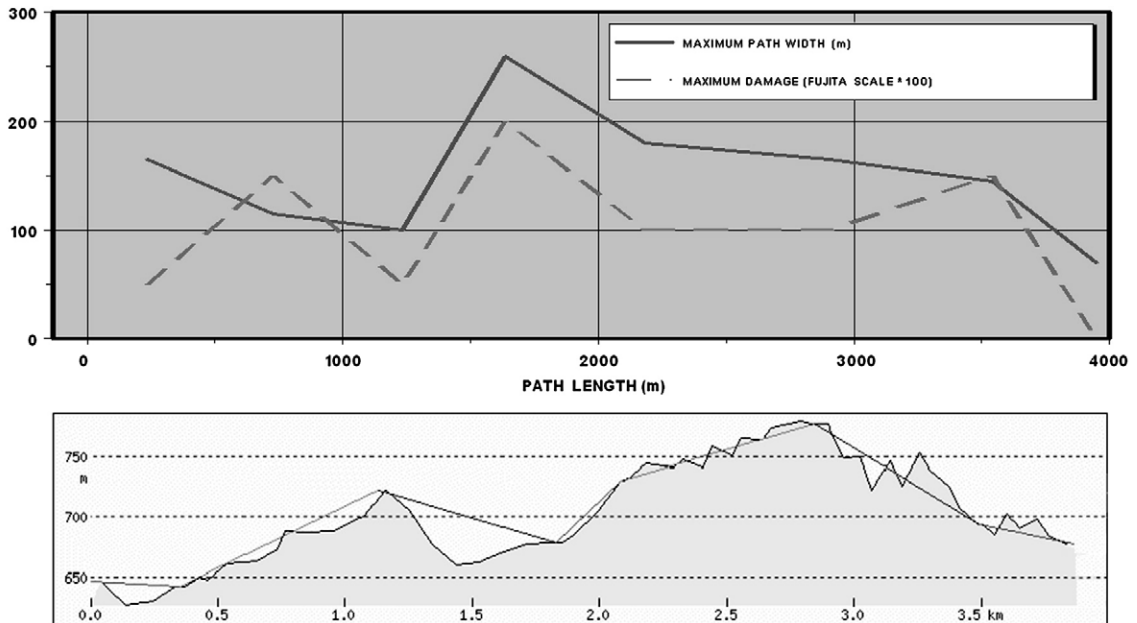


Fig. 9. Schematic evolution of the Castellcir tornado path width and damage intensity (top panel) and the corresponding topographic profile (bottom).

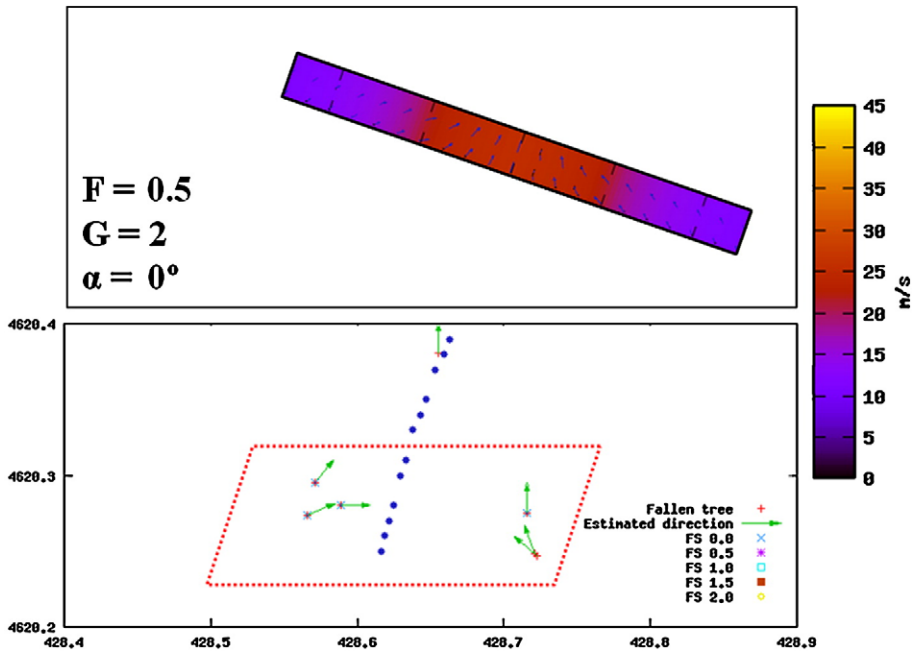


Fig. 10. Theoretical swath pattern (top) suggested from observed tree damage intensities and orientations in the enclosed area (bottom), corresponding to Zone 1. The swath pattern is oriented approximately following the estimated path of the centre of the tornado vortex (dotted line). Vortex parameters (F, G, and α) are displayed in the top panel.

1000 m of the path the Castellcir tornado probably was in the organizing stage; the mature stage corresponded to the path section between 1 and 2 km and the remaining 2 km to the dissipating stage. The terrain altitude might have played some role in the tornado life cycle: the difference between the maximum and minimum height of the path is about 180 m

and the most intense damage and path width took place during a descending slope of 50 m. Though other tornadoes have been described in complex topography environments (see for example Fujita, 1989; Bluestein, 2000; Hannesen et al., 2000; Espejo and Sanz, 2001; Seimon and Bosart, 2004; Giaiotti and Stel, 2007) it is not completely clear the net effect

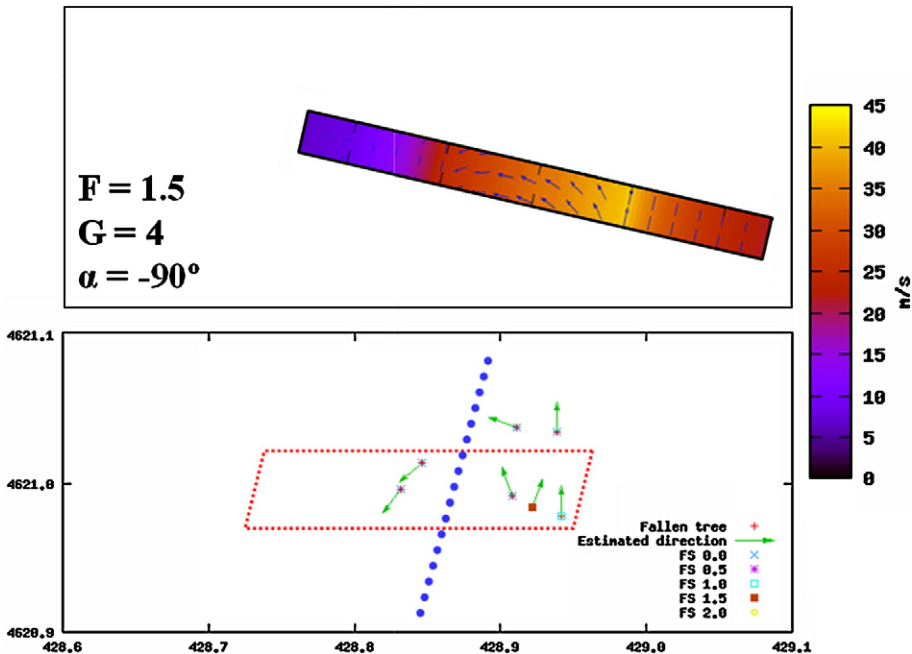


Fig. 11. Similar to Fig. 10, but for Zone 2.

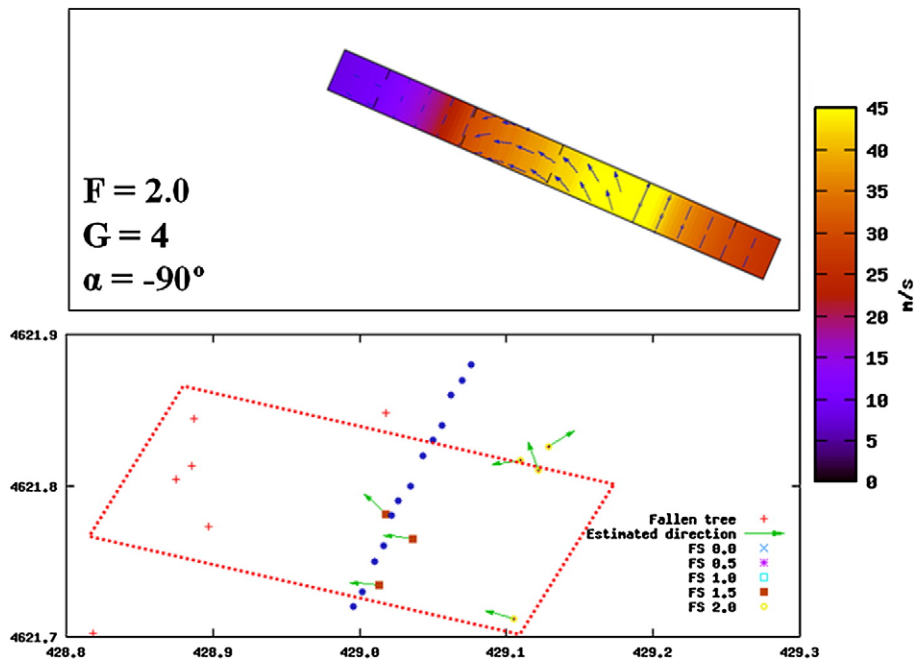


Fig. 12. Similar to Fig. 10, but for Zone 4.

(weakening or intensification) that the topography may have had in this case.

3.4. Swath patterns

The vortex model described in the previous section is used here to complement the analysis of the life cycle of the Castellcir tornado. A careful examination of plots of fallen trees in the different 8 zones described earlier was performed to look for potential similarities with modelled vortex configurations and a selection of comparisons was done.

As an example, Fig. 10 shows a subregion of Zone 1 (lower panel) and a modelled swath pattern. The characteristics of the vortex model are G equal to 2, α equal to 0 and F equal to 0.5; i.e. a weak tornado with predominant inflow circulation (convergent patterns in the tree orientations).

In Fig. 11, it is shown another comparison between observed and modelled swath patterns. In this case, corresponding to Zone 2, there was a clear sign of asymmetry and damage rated as F1.5 was present to the right of the estimated

path centre while only F0.5 damage was found to the left, with tree orientations in the opposite direction. This corresponds to a classical cyclonic tornado pattern; α was equal to -90° (pure tangential flow) though other previous tree orientations suggested an intermediate situation (-45° , not shown). This evolution seems to indicate a transition between the organizing and the mature stage.

Fig. 12, which corresponds to Zone 4, shows a third comparison between modelled and observed fallen trees. This area is where the most intense damage was found (F2.0), also in the right side of the path. Despite the fact that the orientations of the trees found in the left side were not conclusive, it seems plausible that a vortex model with similar characteristics of that shown in Fig. 11, but more intense and wide, could have caused these effects.

A fourth comparison was also performed in Zone 5 (not shown), yielding again a similar swath pattern but smaller and weaker (G equal to 4, α equal to -90° , and F1.0 intensity). Table 1 shows a summary of the details obtained for each Zone, listing cumulated length, maximum path width and damage, α , G and flow type. The tornado life cycle, in terms of the flow circulation derived from ground patterns is similar to that described by Hall and Brewer (1959) though in that case the dissipating stage had a predominant outflow pattern (divergent) not found here.

Table 1

Summary of details of the 8 zones considered in the Castellcir tornado path.

Zone	Cumulated length (m)	Max path width (m)	Max damage (Fujita Scale)	G	Alfa ($^\circ$)	Dominant flow
1	472	165	0.5	2	0	radial inflow
2	984	115	1.5	4	-90	tangential
3	1484	100	0.5	-	-	-
4	1790	260	2.0	4	-90	tangential
5	2574	180	1.0	4	-90	tangential
6	3236	165	1.0	-	-	-
7	3848	145	1.5	-	-	-
8	4048	70	0.0	-	-	-

4. Summary and conclusions

This paper has discussed the application of a methodology to characterize tornado damage in forests based on a simple two dimensional stationary tornado vortex to describe the surface wind field. The basic vortex model is built over the traditional approach of a combined Rankine velocity profile with radial and azimuthal components plus a constant

translational field. Several new additions are considered, such as producing theoretical swath patterns including absolute velocity values (to compare more easily with Fujita damage rating) or using radar data to estimate the translational speed of the vortex. The methodology is demonstrated in the Castellcir tornado that took place in Catalonia (NE Spain) on the 18th October 2006. The site survey indicated a 4 km path and 260 m maximum width as well as F2 damage. Further analysis suggests the existence of three stages in the tornado life cycle. Firstly, an organising stage with predominantly inflow pattern. Secondly a mature stage with maximum damage and width –possibly influenced by the complex topography– with predominant tangential circulation of the vortex. Finally a dissipating stage showing weakening and narrowing of the damage path but no outflow patterns as found in other tornadic cases. The methodology also helped to confirm the tornadic character of the damage discarding possible microbursts in some parts of the area surveyed. The results obtained are consistent with other studies but further work could be devoted to improve the methodology presented. Possible additions include considering more complex velocity profiles (i.e. variable exponents in the radial dependence of velocity) or implementing an automatic comparison between modelled and observed damage to try to optimise the vortex model parameters objectively.

Acknowledgments

We appreciate the constructive comments of two anonymous reviewers which improved the final form of this paper. The authors gratefully acknowledge Marta Aran for her kind help during the preparation and performance of the field work in the Castellcir area. The Meteorological Service of Catalonia provided support for the damage site analysis including the helicopter aerial survey. This study was done under the framework of the Cooperation Agreement (2002) between the Spanish National Meteorological Institute (INM) and the Environment Department which hosts the Meteorological Service of Catalonia.

References

- Aran, M., Amaro, J., Arús, J., Bech, J., Figuerola, F., Gayà, M., Vilaclara, E., 2009. Synoptic and mesoscale diagnosis of a tornado in Castellcir, Catalonia, on 18th October 2006. *Atmos. Res.* 93, 147–160 (this issue). doi:10.1016/j.atmosres.2008.09.31.
- Bech, J., Codina, B., Lorente, J., Bebbington, D., 2003. The sensitivity of single polarization weather radar beam blockage correction to variability in the vertical refractivity gradient. *J. Atmos. Ocean. Technol.* 20, 845–855.
- Bech, J., Vilaclara, E., Pineda, N., Rigo, T., López, J., O'Hora, F., Lorente, J., Sempere, D., Fabregas, F.X., 2004. The weather radar network of the Catalan Meteorological Service: description and applications. *Proc. European Radar Conference*, pp. 416–420.
- Bech, J., Pascual, R., Rigo, T., Pineda, N., López, J.M., Arús, J., Gayà, M., 2007. An observational study of the 7 September 2005 Barcelona tornado outbreak. *Nat. Hazards Earth Syst. Sci.* 7, 129–139.
- Bluestein, H.B., 2000. A tornadic supercell over elevated, complex terrain: the Divide, Colorado, storm of 12 July 1996. *Mon. Weather Rev.* 128, 795–809.
- Bluestein, H.B., 2007. Advances in applications of the physics of fluids to severe weather systems. *Rep. Prog. Phys.* 70, 1259–1323. doi:10.1088/0034-4885/70/8/R01.
- Bluestein, H.B., Lee, W.C., Bell, M., Weiss, C.C., Pazmany, A.L., 2003. Mobile Doppler radar observations of a tornado in a supercell near Bassett, Nebraska, on 5 June 1999. Part II: tornado-vortex structure. *Mon. Weather Rev.* 131, 2968–2984.
- Bluestein, H.B., Weiss, C.C., Pazmany, A.L., 2004. The vertical structure of a tornado near Happy, Texas, on 5 May 2002: high-resolution, mobile, W-band, Doppler radar observations. *Mon. Weather Rev.* 132, 2325–2337.
- Bluestein, H.B., Weiss, C.C., French, M.M., Holthaus, E.M., Tanamachi, R.L., Frasier, S., Pazmany, A.L., 2007. The structure of tornadoes near Attica, Kansas, on 12 May 2004: high-resolution, mobile, Doppler radar observations. *Mon. Weather Rev.* 135, 475–506.
- Brooks, H.E., 2004. On the relationship of tornado path length and width to intensity. *Weather Forecast.* 19, 310–319.
- Bunting, W.F., Smith, B.E., 1993. A guide for conducting damage surveys. NOAA Tech. Memo. NWS SR-146.
- Burgess, D.W., Magsig, M.A., Wurman, J., Dowell, D.C., Richardson, Y., 2002. Radar observations of the 3 May 1999 Oklahoma City Tornado. *Weather Forecast.* 17, 456–471.
- Church, C., Snow, J., Baker, G., Agee, E., 1979. Characteristics of tornado-like vortices as a function of swirl ratio: a laboratory investigation. *J. Atmos. Sci.* 36, 1755–1776.
- Dessens, J., 1972. Influence of ground roughness on tornadoes: a laboratory simulation. *J. Appl. Meteorol.* 11, 72–75.
- Doswell, C.A., Burgess, D.W., 1988. On some issues of United States Tornado Climatology. *Mon. Weather Rev.* 116, 495–501.
- Doswell, C.A. Jr., H.E. Brooks, N. Dotzek, 2007. On the Implementation of the Enhanced Fujita Scale in the USA. Submitted to *Atmos. Res.* [Available at <http://www.essl.org/people/dotzek/papers.htm>].
- Dotzek, N., Peterson, R.E., Feuerstein, B., Hubrig, M., 2008. Comments on "A simple model for simulating tornado damage in forests". *J. Appl. Meteor. Climatol.* 47 (2), 726–731.
- Espejo, F., Sanz, R., 2001. The Teruel tornado of 28 August 1999. V National Forecasting Symposium, INM, Madrid. In Spanish, available from: AEMET, Leonardo Prieto Castro, 8. Ciudad Universitaria. 28040 Madrid, Spain.
- Fujita, T.T., 1981. Tornadoes and downbursts in the context of generalized planetary scales. *J. Atmos. Sci.* 38, 1511–1534.
- Fujita, T.T., 1989. The Teton-Yellowstone Tornado of 21 July 1987. *Mon. Weather Rev.* 117, 1913–1940.
- Gayà, M., 2005. Tornadoes in Spain (1987–2005): temporal and spatial distribution. *Rev. Climatol.* 5, 9–17 (In Spanish, available at: <http://webs.ono.com/usr012/reclim/reclim05b.pdf>).
- Giaiotti, D.B., Stel, F., 2007. A multiscale observational case study of an isolated tornadic supercell. *Atmos. Res.* 83, 152–161.
- Golden, J.H., Purcell, D., 1978. Life cycle of the Union City, Oklahoma Tornado and comparison with waterspouts. *Mon. Weather Rev.* 106, 3–11.
- Grasso, L.D., Cotton, W.R., 1995. Numerical simulation of a tornado vortex. *J. Atmos. Sci.* 52, 1192–1203.
- Hall, F., Brewer, R.D., 1959. A sequence of tornado damage patterns. *Mon. Weather Rev.* 87 (6), 207–216.
- Hannesen, R., Dotzek, N., Handwerker, J., 2000. Radar analysis of a tornado over hilly terrain on 23 July 1996. *Phys. Chem. Earth, Part B Hydrol. Oceans Atmos.* 25 (10–12), 1079–1084.
- Holland, A.P., Riordan, A.J., Franklin, E.C., 2006. A simple model for simulating tornado damage in forests. *J. Appl. Meteor. Climatol.* 45, 1597–1611.
- Kobayashi, F., Kikuchi, K., Uyeda, H., 1996. Life cycle of the Chitose Tornado of September 22, 1988. *J. Meteorol. Soc. Jpn.* 74, 125–140.
- Lee, W.C., Wurman, J., 2005. Diagnosed three-dimensional axisymmetric structure of the Mulhall Tornado on 3 May 1999. *J. Atmos. Sci.* 62, 2373–2393.
- Lewellen, W.S., 1993. Tornado vortex theory. In: Church, C., Burgess, D., Doswell, C., Davies-Jones, R. (Eds.), *The Tornado: Its Structure, Dynamics, Prediction, and Hazards*. *Geophys. Monogr.*, vol. 79. Amer. Geophys. Union, pp. 19–39.
- Mateo, J., Ballart, D., Brucet, C., Aran, M., Bech, J., 2009. A study of a heavy rainfall event and a tornado outbreak during the passage of a squall line over Catalonia. *Atmos. Res.* 93, 131–146 (this issue). doi:10.1016/j.atmosres.2008.09.030.
- Peterson, R.E., 1992a. Johannes Letzmann: a pioneer in the study of tornadoes. *Weather Forecast.* 7 (1), 166–184.
- Peterson, R.E., 1992b. Letzmann's and Koschmieder's "Guidelines for research on funnels, tornadoes, waterspouts and whirlwinds". *Bull. Am. Meteorol. Soc.* 73 (5), 597–611.
- Peterson, C.J., 2000. Damage and recovery of tree species after two different tornadoes in the same old growth forest: a comparison of infrequent wind disturbances. *For. Ecol. Manag.* 135 (1–3), 15,237–15,252.
- Peterson, C.J., Pickett, S.T.A., 1991. Treefall and resprouting following catastrophic windthrow in an old-growth hemlock-hardwoods forest. *For. Ecol. Manag.* 42 (3–4), 205–217.
- Ramis, C., Arús, J., López, J.M., Mestres, A.M., 1997. Two cases of severe weather in Catalonia (Spain), an observational study. *Meteorol. Appl.* 4, 207–217.
- Seimon, A., Bosart, L.F., 2004. An observationally based hypothesis for significant tornadogenesis in mountain environments. Preprints, 22nd Conference On Severe Local Storms, Hyannis, Ma, 4–8 October 2004. Available at <http://ams.confex.com/ams/pdfpapers/82063.pdf>.
- Tanamachi, R.L., Bluestein, H.B., Lee, W.C., Bell, M., Pazmany, A., 2007. Ground-based velocity track display (GBVTD) analysis of W-band Doppler radar data in a tornado near Stockton, Kansas, on 15 May 1999. *Mon. Weather Rev.* 135, 783–800.

- TTU, 2006. A recommendation for an enhanced Fujita Scale (EF-Scale). Wind Science and Engineering Center, Texas Tech University, Lubbock, Texas 79409-1023. 111 pp. [Available on-line at <http://www.wind.ttu.edu/EFScale.pdf>].
- Wakimoto, R.M., Martner, B.E., 1992. Observations of a Colorado Tornado. Part II: combined photogrammetric and Doppler radar analysis. *Mon. Weather Rev.* 120, 522–543.
- Wakimoto, R.M., Murphey, H.V., Dowell, D.C., Bluestein, H.B., 2003. The Kellerville Tornado during VORTEX: damage survey and Doppler radar analyses. *Mon. Weather Rev.* 131, 2197–2221.
- Wegener, A., 1917. *Wind- und Wasserhosen in Europa (Tornadoes in Europe)*. Verlag Friedrich Vieweg und Sohn, Braunschweig. 301 pp. [In German, available on-line at <http://essl.org>, section References].
- Wurman, J., 2002. The multiple-vortex structure of a tornado. *Weather Forecast.* 17, 473–505.
- Wurman, J., Alexander, C., Robinson, P., Richardson, Y., 2007. Low-level winds in tornadoes and potential catastrophic tornado impacts in urban areas. *Bull. Am. Meteorol. Soc.* 88 (1), 31–46.